ISSN 1070-3284, Russian Journal of Coordination Chemistry, 2014, Vol. 40, No. 4, pp. 224–231. © Pleiades Publishing, Ltd., 2014.

Novel 1D Mn(II) Complexes Containing Aromatic Dicarboxylic Acids[1]

D. Zhao[a], T. Shi[a], C. Chen[a], Z. Si[a, *], Q. Duan[a, **], and L. Shi[b]

[a] *School of Materials Science and Engineering, Changchun University of Science and Technology, Changchun, 130022 P.R. China*

[b] *College of Sciences, Zhejiang A & F University, Lin'an, 311300 P.R. China*

*e-mail: * szj@cust.edu.cn; ** danqian88@hotmail.com*

Received April 26, 2013

Abstract—Three Mn(II) complexes of $[MnL(Bipy)(H_2O)]_n$ (**I**), $[Mn_3(Phen)_2(HL)_2(L)_2]_n$ (**II**), and $[Mn(Phen)_2(HL)(OH)]$ (**III**), where L = 4,4'-(2-acetylpropane-1,3-diyl)dibenzoic acid, Bipy = 2,2'-bipyridine, and Phen = 1,10-phenanthroline, were hydrothermally synthesized and characterized by single crystal X-ray diffractions, infrared spectroscopy, thermogravimetric analyses, and magnetic analyses. Complexes **I** and **II** are one dimensional (1D) coordination polymers which can form the supramolecules with the help of the intermolecular hydrogen bond interactions. Finally, the landé factors are simulated by magentochemical analysis to be 2.15 and 1.80 for **I** and **II** with $S = 5/2$, respectively.

DOI: 10.1134/S1070328414030117

INTRODUCTION

Recently, the crystal materials of metal complexes were extensively studied [1–10] due to their potential applications in many fields, such as the magnetic fields catalysis and the molecular recognition. In order to obtain the metal complexes with interesting molecular structures and/or high performances, lots of novel organic compounds [11–17], including polypyridines [11, 12], cyclic ethers [13, 14], and organic acids [15–17], were applied as the coordination ligands. In the last several decades, the metal complexes based on the organic acids appealed most researchers' attentions because the carboxyl groups with several coordination modes of organic acids can act as not only the coordination groups but also the donor and/or acceptors of the hydrogen bonds [18, 19]. There should mainly be two kinds of polycarboxylic acids of the non-aromatic polycarboxylic acids and the aromatic polycarboxylic acids, and they possess different advantages to construct metal complexes: (1) alkyl linkers of the non-aromatic polycarboxylic acids can change their spatial structures to meet the coordination requirements of the metal complexes [20–24]; (2) the aromatic rings can give the aromatic polycarboxylic acids some additional molecular forces, such as π–π stacking and π–H interactions [25, 26]. For example, the non-conjugated aromatic polycarboxylic acids with an atom between the aromatic rings are useful to prepare metal complexes with unexpected structures and/or excellent properties [21, 22]. According to the above mentioned researches, we designed and synthesized an non-conjugated aromatic dicarboxylic acids of 4,4'-(2-acetylpropane-1,3-diyl)dibenzoic acid (H_2L) which have 1,3-propylidene group between the aromatic rings and used it to hydrothermally synthesize three Mn(II) complexes of $[MnL(Bipy)(H_2O)]_n$ (**I**), $[Mn_3(HL)_2(L)_2(Phen)_2]_n$ (**II**), and $[MnL(Phen)_2(H_2O)]$ (**III**) (Bipy = 2,2'-bipyridine and Phen = 1,10-phenanthroline). At last, the X-ray single crystal diffraction, the infrared spectroscopy, thermogravimetric and magnetic analyses were applied to characterize the prepared Mn(II) complexes.

EXPERIMENTAL

Materials and methods. All chemicals and reagents from the commercial sources were used without further purification. IR spectra were recorded on a FTIR-8400S SHIMADZU spectrophotometer in the 4000–400 cm^{-1} region with KBr pellets. The magnetic susceptibility data were collected in the magnetic field of 1000 Oe on a MPMS RSO with the temperature range 2–300 K.

Synthesis of H_2L. The mixture of K_2CO_3 (6.9000 g, 0.050 mol), pentane-2,4-dione (5.1 mL, 0.015 mol), and 50 mL DMF was stirred 1 h, and then the methyl 4-(chloromethyl)benzoate (9.2300 g, 0.050 mol) was dropped into the mixture which was stirred another 24 h. The raw product of dimethyl 4,4'-(2,2-diacetylpropane-1,3-diyl)dibenzoate was collected by the filtration after the mixture was poured into 300 mL H_2O. The precipitate (65.0 mg) and H_2O (3 mL) were sealed in a Teflon-lined stainless autoclave and heated at 170°C for 1 day under autogenous pressure and then

[1] The article is published in the original.

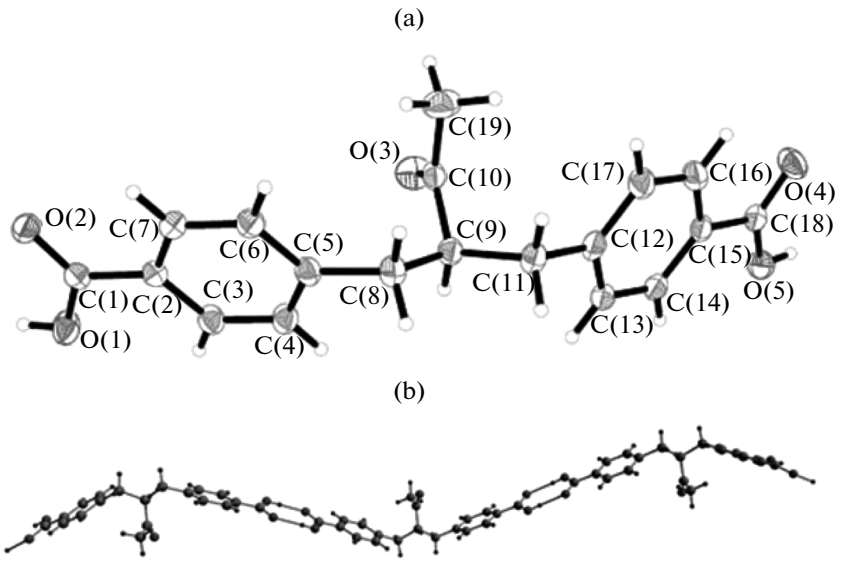

Fig. 1. ORTEP drawing with 30% thermal ellipsoids (a) and the view of 1D superomolecule chain (b) in crystal of H_2L.

cooled to room temperature during 10 h. Colorless prism like crystals of H_2L suitable for X-ray analysis were obtained with yield of ~60.0%.

IR (KBr; ν, cm^{-1}): 3010, 2966, 2667, 2547, 1697, 767. ^1H NMR (400 MHz; δ, ppm): 1.908 (3H, s.), 2.7350 (2H, tetra), 2.943 (2H, tetra), 7.303 (4H, d., $J = 8$), 7.848 (4H, d., $J = 8$), 12.847 (2H, s.).

Synthesis of I. A mixture of $Mn(CH_3COO)_2 \cdot 4H_2O$ (24.5 mg, 0.1 mmol), H_2L (34.0 mg, 0.1 mmol), and Bipy (19.2 mg, 0.1 mmol) was stirred in water (3.0 mL) and the pH of the mixture was adjusted to 6.5 with an aqueous ammonia solution, and then sealed in a 5-mL Telfon-lined stainless-steel container, which was heated to 170°C for 72 h and then cooled to room temperature at a rate of 5°C h^{-1}. Yellow block crystals were obtained with yield of ~49.1%.

IR (KBr; ν, cm^{-1}): 3429, 1607, 1402, 1047, 1018, 928, 764, 619.

Synthesis of II. A mixture of $Mn(CH_3COO)_2 \cdot 4H_2O$ (24.5 mg, 0.1 mmol), H_2L (34.0 mg, 0.2 mmol), and Phen (19.80 mg, 0.1 mmol) was stirred in water (3 mL) and the pH of the mixture was adjusted to ~6.5 with an aqueous ammonia solution, and then sealed in a 5-mL Telfon-lined stainless-steel container, which was heated to 170°C for 72 h and then cooled to room temperature at a rate of 5°C h^{-1}. The yellow block crystals of **II** were obtained with the yield of ~49.0%.

IR (KBr; ν, cm^{-1}): 3492, 1591, 1383, 1279, 1101, 939, 847, 729.

Synthesis of III. A mixture of $Mn(CH_3COO)_2 \cdot 4H_2O$ (24.5 mg, 0.1 mmol), H_2L (34.0 mg, 0.1 mmol), and Phen (37.6 mg, 0.2 mmol) was stirred in water (3.0 mL) and the pH of the mixture was adjusted to 5.5 with an aqueous ammonia solution. It was then sealed in a 5-mL Telfon-lined stainless-steel container, which was heated to 170°C for 72 h and then cooled to room temperature at a rate of 5°C h^{-1}, and yellow block crystals of **III** were obtained with yield of ~48.0%.

IR (KBr; ν, cm^{-1}): 3412, 2395, 1709, 1607, 1468, 1400, 1103, 937, 847, 729, 675.

The crystal structures of H_2L and complexes **I**–**III** of were measured on a Bruker Smart Apex CCD single-crystal diffractometer using MoK_α radiation, λ = 0.7107 Å at 293 K. An empirical absorption correction based on the symmetry-equivalent reflections was applied to the data using the SADABS program. The structures were solved using the SHELXL-97 program [27–29]. The crystal data of H_2L and complexes **I**–**III** are listed in Tabel 1, and the corresponding selective bond distances and the bond angles are given in Table 2. Supplementary material for structures H_2L and **I**–**III** has been deposited with the Cambridge Crystallographic Data Centre (nos. 889123 (H_2L); 826826 (**I**); 826825 (**II**); 826824 (**III**); deposit@ccdc.cam.ac.uk or http://www.ccdc.cam.ac.uk).

RESULTS AND DISCUSSION

The ORTEP view of H_2L single crystal with orthorhombic lattice is presented in Fig. 1a. The dihedral angle between the two benzene groups is 45.606°, which suggests that H_2L belong to the V-shaped aromatic di-boxylate ligand. The hydrogen bond length of O(5)–H(5)···O(2) and O(1)–(1)···O(4) (O···O) should be 2.6969(18) and 2.5635(19) Å, respectively), and these intermolecular hydrogen interactions (make the H_2L molecules) form one dimensional (1D) superomolecular chains (Fig. 1b).

Table 1. Crystallographic data and structure refinement for H_2L and complexes **I**–**III**

Parameter	Value			
	H_2L	**I**	**II**	**III**
Formula	$C_{19}H_{18}O_5$	$[C_{29}H_{30}N_2O_2Mn]_n$	$[C_{100}H_{82}N_4O_{22}Mn_3]_n$	$C_{43}H_{38}N_4O_8Mn$
Fw	326.33	621.49	1856.52	793.72
Crystal system	Orthorhombic	Monoclinic	Monoclinic	Triclinic
Space group	*Pbca*	$P2_1/c$	$P2_1/c$	$P\bar{1}$
a, Å	13.7969(8)	16.3637(12)	14.8316(6)	9.8265(12)
b, Å	7.4214(4)	15.2242(11)	20.3886(8)	13.2648(15)
c, Å	32.1093(18)	11.6726(8)	15.0330(6)	14.8373(17)
α, deg	90	90	90	104.912(2)
β, deg	90	97.3070	100.9570	91.960(2)
γ, deg	90	90	90	95.971(2)
V, Å^3	3287.7(3)	2884.3(4)	4463.0(3)	1855.0(4)
Z	8	4	2	2
ρ_{calcd}, mg/m^3	1.319	1.348	1.381	1.414
μ, mm^{-1}	0.095	0.509	0.495	0.418
F(000)	1376	1212	1922	818
θ Range for collection, deg	1.27–26.01	1.25–25.03	1.40–25.03	1.84–26.7
Reflections collected	16730	14344	22544	10166
Completeness, %	100.0	98.9	99.9	97.0
Data/restraints/parameters	3228/0/217	5043/0/371	7876/0/583	7353/4/505
Goodness-of-fit on F^2	1.028	1.030	1.040	1.028
R_1, wR_2 ($I > 2\sigma(I)$)	0.0419/0.1064	0.0849/0.2417	0.0622/0.1667	0.0805/0.2205
R_1, wR_2 (all data)	0.0613/0.1196	0.1593/0.2978	0.0863/0.1880	0.0923/0.2330

According to the ORTEP view of crystal **I** in Fig. 2a, each Mn^{2+} ion is coordinated by a Bipy, a water molecule and two bridge ligands of L^{2-}, which leads **I** to be 1D zigzag chain with a Mn–Mn distance of 16.364 Å (Fig. 2b). For the distorted octahedral geometry of Mn(1), the distances of Mn(1)–O(1), Mn(1)–O(2), Mn(1)–O(5)$^{\#2}$, Mn(1)–O(6)$^{\#2}$, Mn(1)–N(1), and Mn(1)–N(2) are 2.156(5), 2.119(4), 2.240(5), 2.266(4), 2.243(5), and 2.236(5) Å, respectively, while the bond angles of N(1)Mn(1)N(2), O(5)$^{\#2}$Mn(1)O(6)$^{\#2}$, O(2)Mn(1)N(2), O(1)Mn(1)O(6)$^{\#2}$, and N(1)Mn(1)O(5)$^{\#2}$ are 72.2(2)°, 58.11(16)°, 158.48(19)°, 149.69(19)°, and 147.12(17)°, respectively. The deprotonized carboxyl groups of each L^{2-} present two coordination modes of monodentate and bidentate in **I**. These 1D zigzag chains are linked into a 1D grid chains through the intermolecular hydrogen-bonds (Fig. 2c).

The coordination environment of Mn(II) in crystal **II** is presented in Fig. 3a, and the X-ray crystallographic analysis suggests that the linear trinuclear Mn(II) units of **II**, formed with Mn(1) and two crystallographically equivalent Mn(2) and Mn(2)$^{\#3}$ ions (Fig. 3b), extend into a 1D grid chain with the help of L^{2-} bridges (Fig. 3c). The Mn(2) ion is surrounded by two nitrogen atoms (N(1) and N(2)) of a Phen ligand, two oxygen atom (O(1) and O(3)) from two different L^{2-} ligands and two oxygen atoms (O(5)$^{\#3}$ and O(6)$^{\#3}$) from a chelating carboxyl group of HL^-, while Mn(1) is surrounded six oxygen atoms (O(2), O(2)$^{\#3}$, O(4) and O(4)$^{\#3}$ from 4 individual L^{2-} bridge ligands and O(5)$^{\#3}$ and O(5)$^{\#3}$ from another 2 individual HL^- ligands). These results suggest that the completely

Table 2. Selective bond distances (Å) and bond angles (deg) of H_2L, **I**, **II** and **III**

Bond	*d*, Å	Bond	*d*, Å
		H_2L	
O(2)–C(1)	1.250(2)	O(3)–C(10)	1.197(2)
O(5)–C(18)	1.282(2)	O(4)–C(18)	1.243(2)
O(1)–C(1)	1.270(2)		
		I	
N(1)–Mn(1)	2.243(5)	O(5)–Mn(1)$^{\#1}$	2.240(5)
N(2)–Mn(1)	2.236(5)	O(6)–Mn(1)$^{\#1}$	2.266(4)
O(1)–Mn(1)	2.156(5)	Mn(1)–O(5)$^{\#2}$	2.240(5)
O(2)–Mn(1)	2.119(4)	Mn(1)–O(6)$^{\#2}$	2.266(4)
		II	
O(2)–Mn(1)	2.105(3)	N(2)–Mn(2)	2.259(3)
O(4)–Mn(1)	2.108(3)	O(1)–Mn(2)	2.106(3)
O(5)–Mn(1)	2.226(3)	O(3)–Mn(2)	2.106(3)
Mn(1)–O(2)$^{\#3}$	2.105(3)	Mn(2)–O(5)$^{\#3}$	2.294(3)
Mn(1)–O(4)$^{\#3}$	2.108(3)	Mn(2)–O(6)$^{\#3}$	2.295(3)
Mn(1)–O(5)$^{\#3}$	2.226(3)	O(5)–Mn(2)$^{\#3}$	2.294(3)
N(1)–Mn(2)	2.283(3)	O(6)–Mn(2)$^{\#3}$	2.295(3)
		III	
N(1)–Mn(1)	2.266(3)	N(4)–Mn(1)	2.273(3)
N(2)–Mn(1)	2.256(3)	O(1)–Mn(1)	2.084(3)
N(3)–Mn(1)	2.274(3)	O(3)–Mn(1)	2.148(3)
Angle	ω, deg	Angle	w, deg
		H_2L	
O(4)C(18)O(5)	122.67(17)	O(3)C(10)C(9)	120.65(16)
O(4)C(18)C(15)	118.98(16)	O(2)C(1)O(1)	122.93(17)
O(5)C(18)C(15)	118.35(16)	O(2)C(1)C(2)	121.24(16)
O(3)C(10)C(19)	120.28(18)		
		I	
N(1)Mn(1)O(6)$^{\#2}$	91.81(17)	O(2)Mn(1)N(1)	90.54(19)
N(2)Mn(1)N(1)	72.2(2)	O(2)Mn(1)N(2)	158.48(19)
N(2)Mn(1)O(5)$^{\#2}$	94.06(18)	O(2)Mn(1)O(1)	87.5(2)
N(2)Mn(1)O(6)$^{\#2}$	91.82(17)	O(2)Mn(1)O(5)$^{\#2}$	107.27(18)
O(1)Mn(1)N(1)	117.2(2)	O(2)Mn(1)O(6)$^{\#2}$	101.76(17)
O(1)Mn(1)N(2)	89.1(2)	O(5)$^{\#2}$Mn(1)N(1)	147.12(17)
O(1)Mn(1)O(5)$^{\#2}$	91.61(19)	O(5)$^{\#2}$Mn(1)O(6)$^{\#2}$	58.11(16)
O(1)Mn(1)O(6)$^{\#2}$	149.69(19)		
		II	
O(4)Mn(1)O(5)	89.66(12)	O(3)Mn(2)O(5)$^{\#3}$	108.70(11)
O(2)Mn(1)O(4)	91.97(14)	O(1)Mn(2)O(5)$^{\#3}$	97.49(10)
O(2)$^{\#3}$Mn(1)O(5)	89.63(11)	N(2)Mn(2)O(5)$^{\#3}$	150.80(12)
O(4)$^{\#3}$Mn(1)O(5)	90.34(12)	N(1)Mn(2)O(5)$^{\#3}$	86.87(12)
O(3)Mn(2)O(1)	102.57(12)	O(3)Mn(2)O(6)$^{\#3}$	91.32(11)
O(3)Mn(2)N(2)	87.82(13)	O(1)Mn(2)O(6)$^{\#3}$	154.14(11)
O(1)Mn(2)N(2)	102.28(12)	N(2)Mn(2)O(6)$^{\#3}$	99.93(11)
O(3)Mn(2)N(1)	160.38(13)	N(1)Mn(2)O(6)$^{\#3}$	87.26(11)
O(1)Mn(2)N(1)	86.62(12)	O(5)$^{\#3}$Mn(2)O(6)$^{\#3}$	57.08(10)
N(2)Mn(2)N(1)	73.19(13)		
		III	
O(1)Mn(1)O(3)	89.15(12)	N(2)Mn(1)N(4)	94.80(12)
O(1)Mn(1)N(2)	167.17(13)	N(1)Mn(1)N(4)	94.50(12)
O(3)Mn(1)N(2)	92.83(12)	O(1)Mn(1)N(3)	101.12(12)
O(1)Mn(1)N(1)	93.62(14)	O(3)Mn(1)N(3)	98.82(12)
O(3)Mn(1)N(1)	94.86(12)	N(2)Mn(1)N(3)	91.11(12)
N(2)Mn(1)N(1)	73.59(14)	N(1)Mn(1)N(3)	159.97(13)
O(1)Mn(1)N(4)	85.07(11)	N(4)Mn(1)N(3)	73.56(12)
O(3)Mn(1)N(4)	169.29(12)		

Symmetry codes: $^{\#1}\ x-1, y, z$; $^{\#2}\ x+1, y, z$; $^{\#3}\ -x+2, -y, -z+2$.

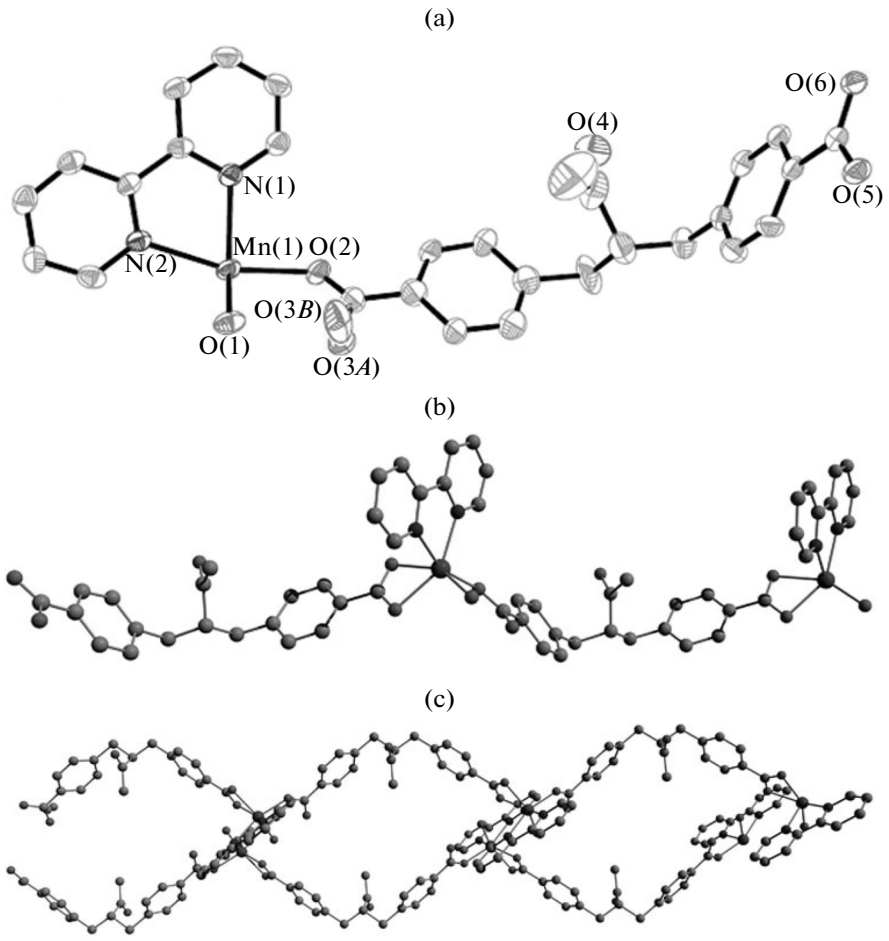

Fig. 2. Coordination environment of Mn(II) atom (a) with 30% thermal ellipsoids and the view of 1D zigzag chain (b) and intermolecular grid chain (c) in crystal of **I**.

deprotonated L^{2-} ligand acts as a bridging bidentate/chelating-bridging tridentate coordination ligand, while the partially deprotonated HL^{-} ligand binds in a chelating-bridging tridentate coordination mode. The above mentioned trinuclear Mn(II) unit, formed with Mn(2), Mn(1), and Mn(2)$^{\#3}$, are linearly located with the distances of 7.002 Å for Mn(2)···Mn(2)$^{\#3}$, and 3.501 Å for Mn(1)···Mn(2) and Mn(1)···Mn(2)$^{\#3}$, respectively. The distances of the Mn(1)–O(2) 2.105(3), Mn(1)–O(4) 2.108(3), and Mn(1)–O(5) 2.226(3) Å are equal to those of Mn(1)–O(2)$^{\#3}$, Mn(1)–O(4)$^{\#3}$ and Mn(1)–O(5)$^{\#3}$, respectively. Bond angles of OMn(1)O are in the range of 88.03(14)°–91.97(14)°. According to Mn(2) atom, the distances of Mn(2)–O(1), Mn(2)–O(3), Mn(2)–O(5)$^{\#3}$, and Mn(2)–O(6)$^{\#3}$ are 2.106(3), 2.106(3), 2.294(3), and 2.295(3) Å, respectively, and Mn(2)–N(1) and Mn(2)–N(2) are 2.283(3) and 2.259(3) Å, respectively. The bond angles of O(3)Mn(2)N(1), N(2)Mn(2)O(5)$^{\#3}$, O(1)Mn(2)O(6)$^{\#3}$, N(2)Mn(2)N(1), and O(5)$^{\#3}$Mn(2)O(6)$^{\#3}$ are 160.38(13)°, 150.80(12)°, 154.14(11)°, 73.19(13)°, and 57.08(10)°, respectively, and other bond angles of OMn(2)O and NMn(2)O are in the range of 86.62(12)°–108.70(11)°. These data suggest that the geometry of the octahedron-coordinated on Mn(2) are more seriously distorted than that on Mn(1). The neighboring trinuclear units are linked by two bridge L^{2-} ligands to form a ring structure and further form a 1D grid chains which are connected to be a 2D rectangular grid framework by the hydrogen-bonding interactions between the HL^{-} ligands. At last, the 2D frameworks form a 3D architecture through the C–H···O hydrogen bonds and weak C–H···π interactions.

The ORTEP view of crystal **III** is presented in Fig. 4a. The Mn^{2+} ion is coordinated by two Phen, one HL^{-}, and one OH^{-} anion. The distances of Mn(1)–N(Phen) range from 2.254(3) to 2.274(3) Å, and the O(1)–Mn(1)(HL^{-}) and O(3)–Mn(1)(OH^{-}) are 2.084(3) and 2.148(3) Å, respectively. The bond angles of O(1)Mn(1)N(2), O(3)Mn(1)N(4), N(1)Mn(1)N(3), N(2)Mn(1)N(1), and N(4)Mn(1)N(3) are 167.17(13)°, 169.29(12)°, 159.97(13)°, 73.59(14)°, and 73.56(12)°, respectively, and other bond angles are

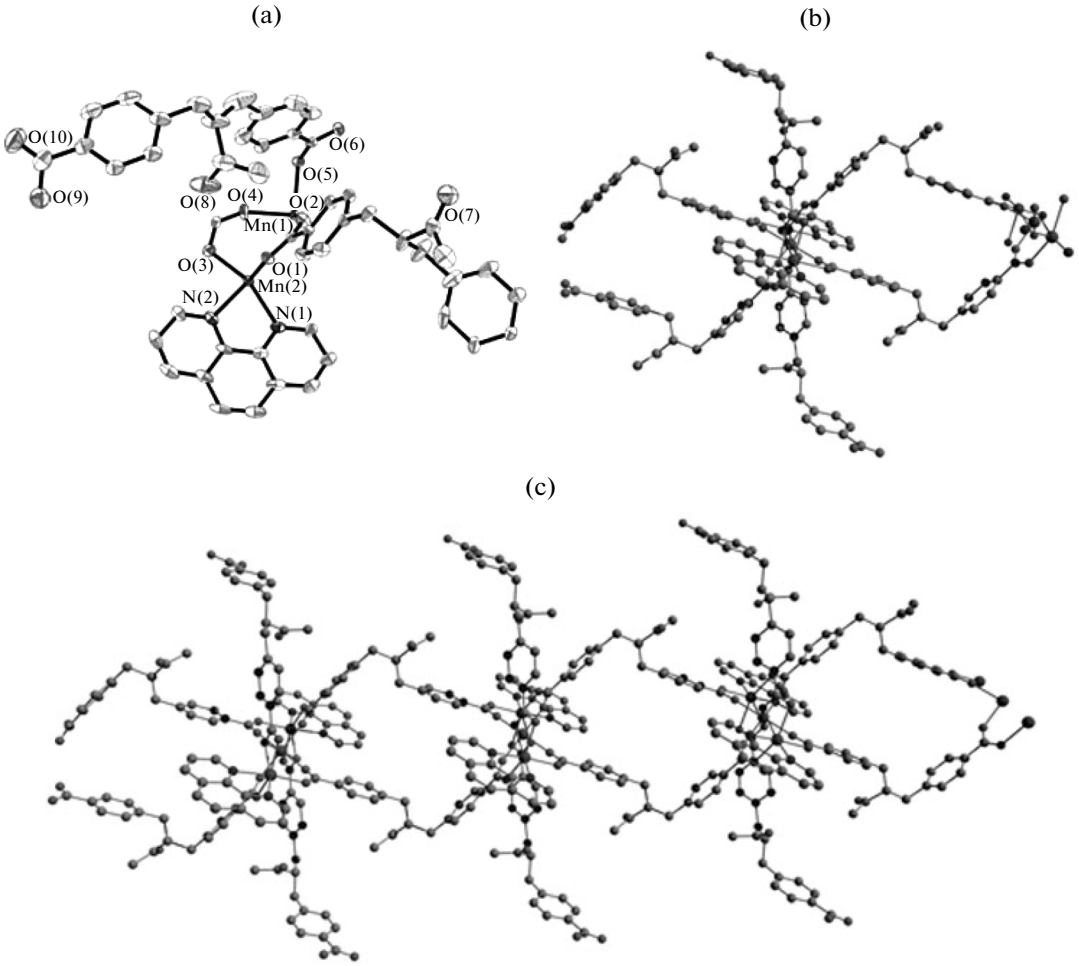

Fig. 3. Coordination environment of Mn(II) atom with 30% thermal ellipsoids (a) and the view of the trinuclear Mn(II) units (b) and 1D grid chain (c) in crystal of **II**.

in the range of 85.07(11)°–101.12(12)°. The O(1)(OH^-) and O(5)(HL^-) form a intermolecular hydrogen interaction with the distance of 2.644 Å which leads to the double molecules based supramolecules (Fig. 4b). These supramolecules are further linked to be 1D chains (Fig. 4c) by the intermolecular hydrogen bond interactions of O(6)–O(7)–O(6)' and O(6)–O(7)'–O(6)', where O(7) (O(7)') and O(6) (O(6)') are supplied by the solvent water and the non-coordinated carboxyl group of HL^-, respectively. The disorder of the formyl and the methine groups of HL^- should be attributed to the thermal vibration.

The thermal gravimetric analysis (TGA) of **I**–**III** were carried out under N_2 atmosphere in the range of 50–800°C to study their thermal stability. The solvent water in the crystals of **I**–**III** should be totally evaporated when the temperature is higher than 130°C. The coordination water of **I** and **II** begin to decompose when the samples are heated up to ~210°C. The decomposition of the organic ligands of **I**, **II**, and **III** begin to dramatically dissociate or sublimate at ~316, ~248, and ~400°C, respectively, and totally decomposed at ~683.0, ~613.0, and ~651.8°C, respectively.

The plots of the χ_m and $1/\chi_m$ versus T of **I** and **II** are depicted in Fig. 5. Fitting the plot of the χ_m versus temperature with the Curie–Weiss law, $\chi_m = C/(T - \theta)$, yields a Curie constant C of 5.09 cm^3 K mol^{-1} (g = 2.157, $S = 5/2$) with a Curie temperature θ of –14.62 K for **I**. The $T\chi_m$ of **I** at 300 K is 3.29 K cm^3/mol which is slightly smaller than the expected value of 4.735 K cm^3/mol for the isolated Mn^{2+} ions ($g = 2$, $S = 5/2$). By fitting the plot of the χ_m versus temperature with the Curie–Weiss law for complex **II**, the constants of C and θ are simulated to be 10.6 cm^3 K mol^{-1} (g = 1.80, $S = 5/2$) and 0.528 K. The $T\chi_m$ of **II** was measured at 300 K to be 10.33 K cm^3 mol^{-1} which is smaller than the expected value of 14.205 K cm^3 mol^{-1} for three isolated Mn^{2+} ions ($g = 2$, $S = 5/2$). These data suggest that there should be week antiferromaganic coupling in complex **I** and **II** [10, 30, 31].

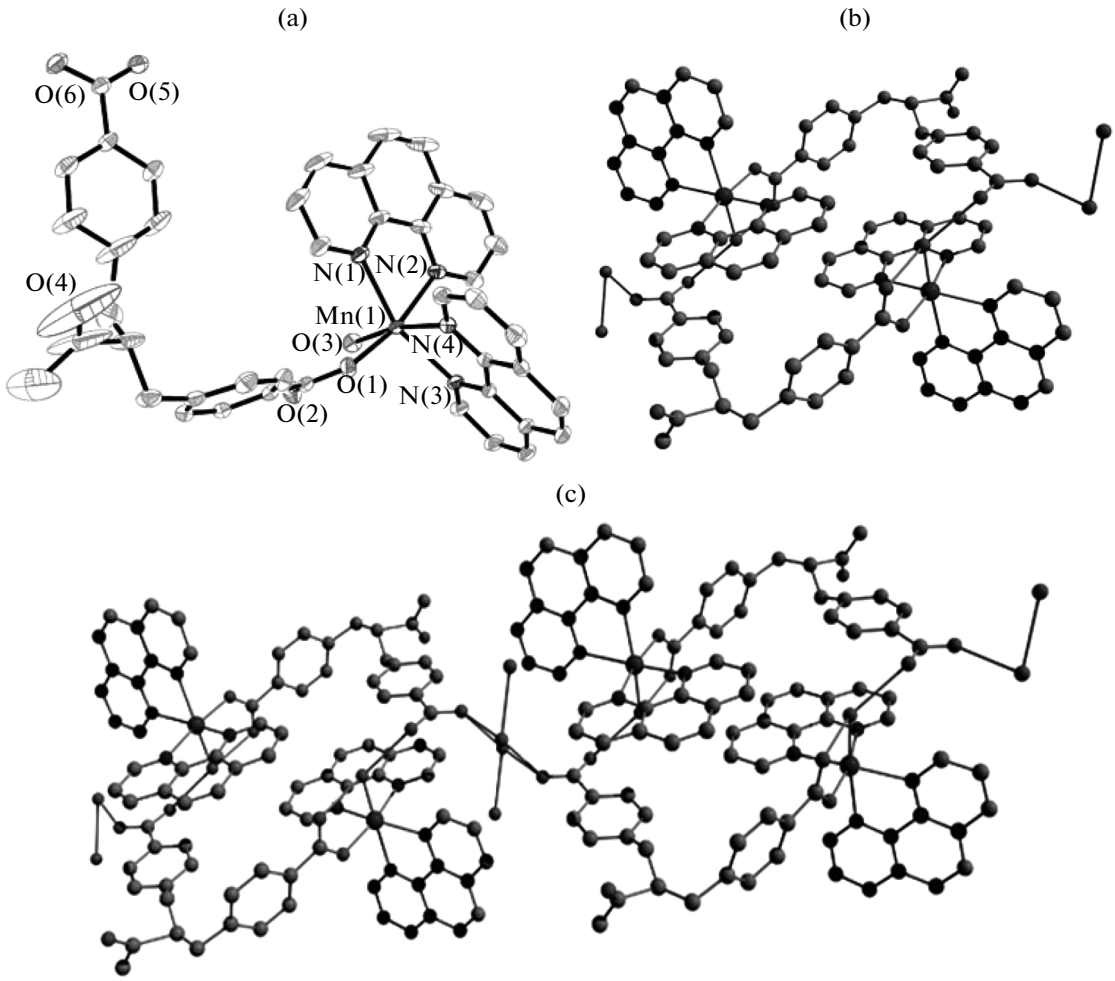

Fig. 4. Coordination environment of Mn(II) atom with 30% thermal ellipsoids (a) and the view of the trinuclear Mn(II) units (b) and 1D grid chain (c) in crystal of **III**.

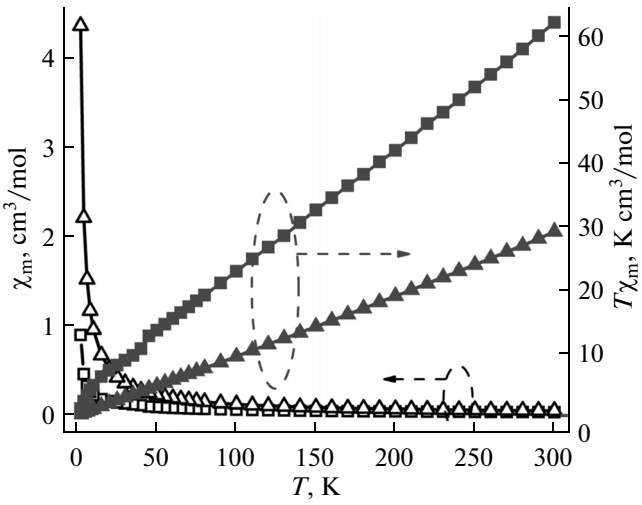

Fig. 5. Magnetic properties of **I** (triangle) and **II** (square) in the form of χ_m versus T and $T\chi_m$ versus T.

ACKNOWLEDGMENTS

The authors are grateful to financial aid from the National Natural Science Foundation of China (grants nos. 20901011 and 21271033) and Natural Science Foundation of Zhejiang Province (grant no. LY12B02013).

REFERENCES

1. Suh, M.P., Park, H.J., Prasad, T.K., and Lim, D.W., *Chem. Rev.*, 2012, vol. 112, p. 782.
2. Rowsell, J.L.C. and Yaghi, O.M., *Angew. Chem. Int. Ed.*, 2005, vol. 44, p. 4670.
3. Nouar, F., Eubank, J.F., Bousquet, T., et al., *J. Am. Chem. Soc.*, 2008, vol. 130, p. 1833.
4. Forgan, R.S., Sauvage, J.-P., and Stoddart, J.F., *Chem. Rev.*, 2011, vol. 111, p. 5434.
5. Wang, X.S., Ma, Sh.Q., Sun, D.F., et al., *J. Am. Chem. Soc.*, 2006, vol. 128, p. 16474.
6. Wang, X.Y., Wang, L., and Wang, Z.M., *Chem. Mater.*, 2005, vol. 17, p. 6369.

7. Leong, W.L. and Vittal, J.J., *Chem. Rev.*, 2011, vol. 111, p. 688.
8. Lin, X.A., Black, J., Wilson, C., et al., *J. Am. Chem. Soc.,* 2006, vol. 128, p. 10745.
9. Zhao, X., Xiao, B., Fletcher, A.J., et al., *Science*, 2004, vol. 306, p. 1012.
10. Chu, Q., Su, Z., Fan, J., et al., *Cryst. Growth Des.*, 2011, vol. 11, p. 3885.
11. Tong, G.S.M., Law, Y.C., Kui, S.C.F., et al., *Chem. Eur. J.*, 2010, vol. 16, p. 6540.
12. Tong, J., Yu, S.-Y., and Li, H., *Chem. Commun.*, 2012, vol. 48, p. 5343.
13. Kim, J.I., Kwak, H.Y., Yoon, J.H., et al., *Inorg. Chem.*, 2009, vol. 48, p. 2956.
14. Gillett-Kunnath, M.M., Paik, J.I., Jensen, S.M., et al., *Inorg. Chem.*, 2011, vol. 50, p. 11695.
15. García-Zarracino, R. and Höpfl, H., *Angew. Chem.*, 2004, vol. 116, p. 1533.
16. García-Zarracino, R. and Höpfl, H., *J. Am. Chem. Soc.*, 2005, vol. 127, p. 3120.
17. Kitagawa, S., Kitaura, R., and Noro, S., *Angew. Chem. Int. Ed.*, 2004, vol. 43, p. 2334.
18. Li, H., Eddaoudi, M., O'Keeffe, M., and Yaghi, O.M., *Nature,* 1999, vol. 402, p. 276.
19. de Lill, D.T., Gunning, N.S., and Cahill, C.L., *Inorg. Chem.,* 2005, vol. 44, p. 258.
20. Lan, Y.Q., Li, S.L., Shao, K.Z., et al., *Cryst. Growth Des.,* 2008, vol. 8, p. 3490.
21. Liu, J.Q., Wang, Y.Y., Zhang, Y.N., et al., *Eur. J. Inorg. Chem.*, 2009, p.147.
22. Chen, X.L., Guo, L., Hu, H.M., et al., *Eur. J. Inorg. Chem.*, 2008, p. 239.
23. Li, N., Chen, L., Lian, F.Y., et al., *Inorg. Chim. Acta,* 2010, vol. 363, p. 3291.
24. Xiao, D.R., Wang, E.B., An, H.Y., et al., *Chem. Eur. J.,* 2006, vol. 12, p. 6528.
25. Zhou, Z.H., Yang, J.M., and Wan, H.L., *Cryst. Growth Des.*, 2005, vol. 5, p. 1825.
26. Wei, Y.Q., Yu, Y.F., Sa, R.J., et al., *CrystEngComm*, 2009, vol. 11, p. 1054.
27. Sheldrick, G.M., *SHELXTL*, *Version 5.10*, Madison (WI, USA): Siemens Analytical X-ray Instruments Inc., 1998.
28. *SMART and SAINT*, Madison (WI, USA): Siemens Analytical X-ray Instruments Inc., 1995.
29. Sheldrick, G.M., *SADABS*, Göttingen (Germany): Univ. of Göttingen, 1996.
30. Zhao, J.P., Hu, B.W., Zhang, X.F., et al., *Inorg. Chem.*, 2010, vol. 49, p. 11325.
31. Malaestean, I.L., Kravtsov, V.C., Speldrich, M., et al., *Inorg. Chem.*, 2010, vol. 49, p. 7764.